1Pb6-1

Examination of amplitude and phase fluctuation of reflected waves from the sea surface by impulse response analysis

Ai Murata and Hiroyuki Hachiya (Tokyo Tech)

1. Introduction

Various studies have been conducted on the fluctuation characteristics of reflected waves from the sea surface. In previous studies1), we proposed effective sea surface roughness that can describe the amplitude fluctuation characteristics of reflected waves regardless of the wavelength of the sea surface. However, quantitative studies based on physical interpretation are not sufficient. In this study, based on the Brettschneider-Mitsuyasu spectra observed deep off the coast of Japan, we investigated the variability of reflected sound waves on the sea surface using impulse response analysis.

2. Calculation method

2.1 Wave generation

In order to reproduce actual sea surface, we used Bretshneider-Mitsuyasu wave spectrum. This spectrum is given by

$$S(f) = 0.257 H_{1/3}^2 T_{1/3} (T_{1/3} f)^{-5} \exp[-1.03 (T_{1/3} f)^{-4}],$$

where f is frequency, $H_{1/3}$ and $T_{1/3}$ are the significant wave height and significant wave period, respectively. By discretizing this spectrum for f and giving random initial phase to each frequency component, we expressed actual sea surface.

2.2 Impulse response from infinite plane strips

In the analysis, we consider impulsive response from a plane strip as shown in **Fig. 1**[2]. We assume that this plane continues infinitely in the y direction. When the source and receiver are at Q on the z axis, and $x_1 > 0$ and $x_2 > 0$, the impulse response signal $u(Q)$ is

$$u(Q) = R \frac{z}{\pi c^2} [D_1(t) - D_2(t)]$$

when $x_1 < 0$ and $x_2 > 0$

$$u(Q) = R \left[\frac{\delta(t - T_z)}{2z} - \frac{z}{\pi c^2} D_1(t) - \frac{z}{\pi c^2} D_2(t) \right]$$

where R is the reflection coefficient, z is the z coordinate of the source and receiver, and c is the speed of sound. $D_1(t)$ and $D_2(t)$ express the reflection from each boundary. $D_1(t)$, the reflection from the edge at x_1, is calculated according to the following equation.

$$D_1(t) = \frac{2T_x}{t(t^2 + T_x^2 - T_1^2)(t^2 - T_1^2)^{1/2}} \quad \text{for } t > T_1$$
$$= 0 \quad \text{for } t < T_1,$$

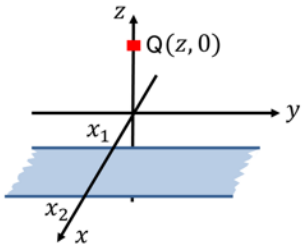

Fig. 1 A plane strip

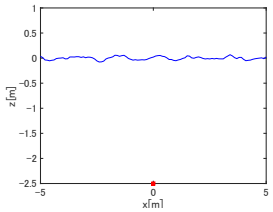

Fig. 2 Wave shape on sea surface

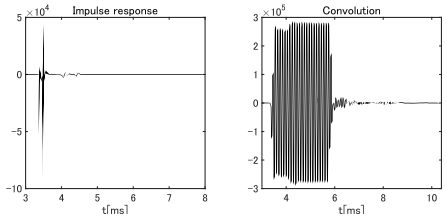

Fig. 3 Impulse response and convolution

where $T_x = \frac{2x_1}{c}$, $T_z = \frac{2z}{c}$, $T_1^2 = T_x^2 + T_z^2$. $D_2(t)$ is calculated similarly. Even if the plane strip is not on the xy plane, we can calculate the impulsive response by rotating and translating the coordinates so that the reference coordinate system contains the strip. With these methods, impulsive response of a rough surface like sea level can be calculated by regarding it as the connection of a number of individual plane strips. Furthermore, convoluting the impulsive response and a burst wave, we can obtain a reflected burst wave signal. **Fig. 2** shows a generated wave surface and the position of the sound source and receiver. The origin is right above the source. The range of the sea surface is x : -5~5 m, and the source depth is 2.5 m. $H_{1/3}$ and $T_{1/3}$ in Fig. 2 are 0.1 m and 1 s. **Fig. 3** shows the impulsive response from the sea surface in Fig. 2 and the result of convolution. The frequency of the burst wave is 10 kHz and the burst length is 2.4 ms. In this study, we changed the wave height and length by controlling values of $H_{1/3}$ and $T_{1/3}$, and observed the amplitude and phase fluctuation.

3. Observation of impulsive response

We generated six sea surfaces that have different wave heights and lengths. Each sea surface is changed as a function of time for 50 s, and we obtained 250 wave surface shapes at every 0.2 s. Using these surfaces, we calculated impulse responses and convolutions for each surface. The six figures in Fig. 4 are overlays of 250 impulse responses for six different sea surfaces. Here, σ_z is the standard deviation of the wave height. k is the wavenumber and Λ is wavelengths of sea surfaces. Red dotted lines indicate the time when the reflected wave returns from the flat sea surface. The amplitude and time fluctuation becomes larger according to the increase of $2k\sigma_z$ and the decrease of Λ. Many signals concentrate around the red dotted line when Λ is long, while in case of small $2k\sigma_z$ most of large signals are after the red line. These characteristics can be explained by Fig. 5. When computing impulsive responses, especially large signals occur at planes orthogonal to acoustic ray paths. In Fig. 5, positions of these orthogonal planes on 250 sea surfaces are plotted by red asterisks. The range of red marks is wider when $2k\sigma_z$ is large and Λ is short. This denotes in such condition large reflections at points far from the origin return late, so that the time and amplitude of impulsive response fluctuates. When the $2k\sigma_z$ becomes larger, red marks distribute a little wider on the vertical direction. We can see that the gathering of large impulsive signals around the red dotted line results from flat and smooth surfaces near the origin moving vertically.

4. Comparison with the FDTD results

We calculated the amplitude and phase by quadrature demodulation of the convoluted signals. In Fig. 6, 250 data are plotted in complex plane. It can be seen that the amplitude fluctuation is smaller than the phase fluctuation when Λ is large. Fig. 7 shows the results of our prior study using FDTD method in same conditions[1]. Distribution patterns in Fig.6 agree well with the FDTD results in Fig. 7.

5. Conclusion

We calculated impulsive responses and reflected sound waves from the sea surface, and observed the relationship with the wave height and length. It was seen that the sea range that influences amplitude fluctuation become wider when $2k\sigma_z$ is large and Λ is short. Also we compared with the FDTD results, and confirmed that characteristics of the amplitude and phase fluctuation are about the same.

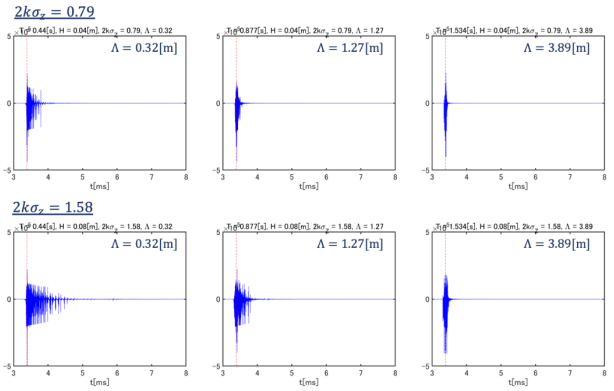

Fig. 4 Impulsive responses

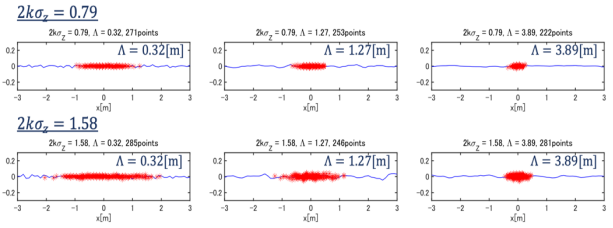

Fig. 5 Positions of orthogonal planes

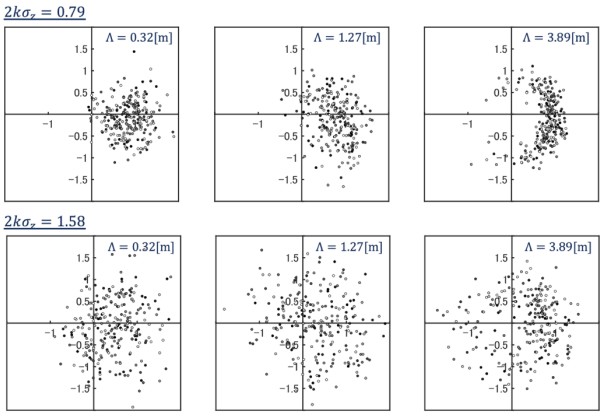

Fig. 6 Convolved signals on complex planes

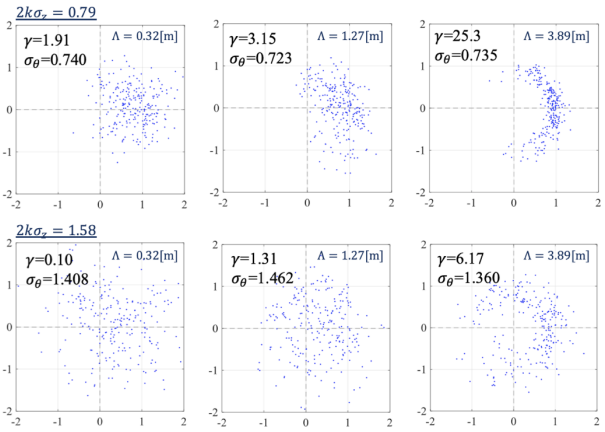

Fig. 7 FDTD results on complex planes[1]

References

1. T. Tsukui, S. Hirata, and H. Hachiya : Jpn. J. Appl. Phys. 61, SG1078 (2022).
2. C. S.Clay, H. Medwin, *Acoustical Oceanography*, John Wiley & Sons, 1977.